

University of Groningen

## Effects of impurities on subsurface CO<sub>2</sub> storage in gas fields in the northeast Netherlands

Bolourinejad, Panteha

**IMPORTANT NOTE:** You are advised to consult the publisher's version (publisher's PDF) if you wish to cite from it. Please check the document version below.

*Document Version*

Publisher's PDF, also known as Version of record

*Publication date:*

2015

[Link to publication in University of Groningen/UMCG research database](#)

*Citation for published version (APA):*

Bolourinejad, P. (2015). *Effects of impurities on subsurface CO<sub>2</sub> storage in gas fields in the northeast Netherlands*. [Thesis fully internal (DIV), University of Groningen]. University of Groningen.

### Copyright

Other than for strictly personal use, it is not permitted to download or to forward/distribute the text or part of it without the consent of the author(s) and/or copyright holder(s), unless the work is under an open content license (like Creative Commons).

The publication may also be distributed here under the terms of Article 25fa of the Dutch Copyright Act, indicated by the "Taverne" license. More information can be found on the University of Groningen website: <https://www.rug.nl/library/open-access/self-archiving-pure/taverne-amendment>.

### Take-down policy

If you believe that this document breaches copyright please contact us providing details, and we will remove access to the work immediately and investigate your claim.

Downloaded from the University of Groningen/UMCG research database (Pure): <http://www.rug.nl/research/portal>. For technical reasons the number of authors shown on this cover page is limited to 10 maximum.

## Chapter 5



### **Experimental investigation of porosity and permeability variations in reservoirs and caprock following co-injection of sulphur dioxide and hydrogen sulfide with carbon dioxide**

**Based on publication in:**

Bolourinejad, P. and Herber, R. (2015) Experimental investigation of porosity and permeability variations in reservoirs and caprock following co-injection of sulfur dioxide and hydrogen sulfide with carbon dioxide. *Journal of Petroleum Science and Engineering* 129, 137-144.

## Chapter 5

---

### 5 Experimental investigation of porosity and permeability variations in reservoirs and caprock following co-injection of sulphur dioxide and hydrogen sulfide with carbon dioxide

#### Abstract

Carbon dioxide (CO<sub>2</sub>) capture, transport and storage (CCTS) in deep geological formations can mitigate the atmospheric concentration of greenhouse gases. Purity of this gas is an important aspect for CCTS since it drives up the cost of capture. When leaving some impurities from the flue gas in the CO<sub>2</sub> stream, a cost reduction may be achieved but the risks at transport and storage may increase. In order to investigate the effects of the possible impurities (H<sub>2</sub>S and SO<sub>2</sub>) in the CO<sub>2</sub> stream during subsurface storage laboratory experiments were performed on Permian Rotliegend reservoir and Zechstein cap rock core samples from gas fields in northeast Netherlands. The rock samples were subjected for 30 days to static in situ conditions (300 bar, 100°C) in the presence of brine and an injected gas mixture of CO<sub>2</sub> +100 ppm SO<sub>2</sub> + 100 ppm H<sub>2</sub>S. Following injection of the mixture permeability of the reservoir and caprocks increased by a factor of 1.02-1.9 and 1.2-3.1, respectively. Although an enhanced level of anhydrite precipitation was observed, the increase in permeability of the samples show that dissolution of carbonate, feldspar and kaolinite minerals is dominant. In addition it was shown that the initial porosity-permeability relation of the samples remains valid to predict the behavior of the reservoir after injection of the gas mixture. For the caprock, the precipitation of anhydrites results in a less enhanced permeability than in the case of injection of pure CO<sub>2</sub>. This may lead to the conclusion that the addition of low quantities (100 ppm) of SO<sub>2</sub> and H<sub>2</sub>S in CO<sub>2</sub> during subsurface storage does not increase the risk of leakage through the Zechstein caprock more than when using pure CO<sub>2</sub>.

**Keywords:** CO<sub>2</sub> storage, impurities, porosity, permeability, mineralization, Rotliegend, Zechstein

#### 5.1 Introduction

The increasing concentration of greenhouse gas (GHG) in the atmosphere is a strong driver for development of new mitigating methods and technologies (Battistelli and Marcolini, 2009; IPCC, 2005). Anthropogenic carbon dioxide (CO<sub>2</sub>) emission forms the largest contribution to rising GHG concentrations (IPCC, 2005). CO<sub>2</sub> capture from point sources (e.g. fossil fuelled power plants) and storage in geological formations such as saline aquifers, depleted oil and gas fields and coal seams is a potential means to reduce CO<sub>2</sub> emissions (Audigane et al., 2007b; Palandri and Kharaka, 2005). Candidate geological formations for storage should have sufficient capacity, appropriate injectivity and be sealed by a layer of an impermeable caprock (Bos, 2007). In addition, the ability to predict both short and long term effects of CO<sub>2</sub> on geological formations is a necessity for successful application (Balashov et al., 2013).

In general, CO<sub>2</sub> from power plants is not pure and contains various types of impurities (e.g. H<sub>2</sub>S, SO<sub>2</sub>, NO<sub>x</sub>, H<sub>2</sub>, Ar, CO and NH<sub>3</sub>) (Wilke et al., 2012). It is estimated that 75% of the Carbon Capture and Storage (CCS) cost is related to the separation of CO<sub>2</sub> from the flue gas (IPCC, 2005; Ji and Zhu, 2013). The injection of CO<sub>2</sub> along with some of the impurities can help to save energy and cost in the capture process. However this might increase the risks related to the transport and storage (Ji and Zhu, 2013). Hence it is vital to study the additional impact of these impurities (type and concentration) on transportation system and storage site.

In the case of transport of CO<sub>2</sub> the presence of impurities can lead to phase separation, hydrate formation and corrosion (Bolourinejad and Herber, 2014; IPCC, 2005). At the storage site, impurity of CO<sub>2</sub> may affect well integrity and injectivity as well as long-term cap-rock seal integrity and hence risk of leakage. Many researchers studied impacts of different impurities on geological formations both experimentally and with the help of modelling software such as PHREEQC (Parkhurst, and Appelo, 2013), TOUGHREACT (Xu et al., 2004) and CMG-GEM (CMG, 2011).

Wilke et al., (2012) performed experiments (77 bars, 49° C, duration 42 days) with pure and impure (0.5% NO<sub>2</sub> or SO<sub>2</sub>) CO<sub>2</sub> injection on single mineral phases (albite, microcline, calcite, dolomite, anhydrite, kaolinite and biotite). Co-injection of NO<sub>2</sub> and SO<sub>2</sub> resulted in the formation of nitric and sulfuric acid respectively and caused a stronger pH reduction than in the pure CO<sub>2</sub> scenario due to the formation of carbonic acid formation. In their CO<sub>2</sub>-NO<sub>2</sub> experiment they reported a 50 wt% dissolution of anhydrite and associated precipitation of gypsum. Palandri et al. (2005) investigated CO<sub>2</sub>-SO<sub>2</sub> reactions with hematite (300 bar, 150 °C) resulting in the formation of pyrite, siderite and elemental sulfur. Palandri and Kharaka, (2005) mentioned that in a representative flue gas mixture (e.g. <1% SO<sub>2</sub>) there is not sufficient reducing agent (e.g. H<sub>2</sub>S and SO<sub>2</sub>) to reduce all of the iron and no siderite can be formed. Hence, the targeted reservoir rock should contain other metals than Fe in order to make carbonate precipitation possible and trap all of the CO<sub>2</sub> as a mineral. Parmentier et al., (2013) performed a 30 day experiment on calcite minerals by injection of pure SO<sub>2</sub> and showed both calcite dissolution and anhydrite precipitation. Bachu and Bennion, (2009) investigated the impact of impurities (H<sub>2</sub>S, SO<sub>2</sub>, CH<sub>4</sub> and N<sub>2</sub>) in the CO<sub>2</sub> stream. They showed that the impurities would, due to their differences in solubility, chromatographically partition at the front end of the gas plume advancing through the water-saturated porous medium. Koenen et al., (2011a) modelled both short and long term effects of impure CO<sub>2</sub> injection in the presence of multiple impurities such as SO<sub>2</sub>, H<sub>2</sub>S, N<sub>2</sub> in a depleted gas field in the Netherlands. Using PHREEQC modeling software they concluded that the short-term effects of impurities are insignificant compared to that of pure CO<sub>2</sub>. In the long-term, presence of impurities leads to a minor difference in mineralogy (precipitation of new mineral phases) when compared to pure CO<sub>2</sub> injection. Waldmann et al., (2013a) used similar software and modelled SO<sub>2</sub> co-injection in Triassic Buntsandstein. The results showed an increase in K-feldspar dissolution next to anhydrite precipitation.

In our research project the impact of various impurities on subsurface storage of CO<sub>2</sub> was studied both experimentally. The experiments were carried out on Permian Rotliegend reservoir and Zechstein caprock core samples from depleted gas fields. The use of actual core samples rather than using a single mineral phase enabled us to measure porosity and permeability of the samples pre and post experiments. In a previous paper (Bolourinejad and Herber, 2014) the impact of injection of pure CO<sub>2</sub> and also co-injection of CO<sub>2</sub> + 100 ppm H<sub>2</sub>S were already discussed. In the current article the focus is on the subsurface storage of CO<sub>2</sub> in combination with a mixture of 100 ppm SO<sub>2</sub> and 100 ppm H<sub>2</sub>S. The objective is to assess to which degree the impact of a combination of sulfur gasses on the reservoir is different from that of the individual components. The geochemical impact of the gas mixtures is experimentally evaluated on reservoir as well as caprock core samples at in-situ subsurface pressure and temperature conditions as encountered in gas fields in northeast Netherlands. In order to simulate the local subsurface conditions as much as possible, a small (2%) methane component is included in the mixture although the chemical interaction between the impurities and methane is very limited. Prior to the experiments, the mineralogical composition of the samples is determined with X-Ray Diffraction (XRD) and Scanning Electron microscopy (SEM). After the experiments, the change in the mineral composition was monitored by SEM. Brine samples were also collected and analyzed by Induced Coupled Plasma-Optical Emission Spectroscopy (ICP-OES) techniques. Furthermore, after the experiments the porosity of the samples was measured to establish whether the initial porosity-permeability relationship in the reservoirs still holds after injection and thus can be utilized for post-injection scenarios.

## **5.2 Methods and Materials**

### **5.2.1 Sampling**

The core samples for Permian Rotliegend sandstone reservoir and Permian Zechstein anhydrite/carbonate caprock were obtained from wells in northeast Netherlands. Depth range of the selected samples is between 2.8 – 3.2 km and their porosity varies between 0.3 and 22% while permeability ranges between 0.005 mD and 459 mD. The samples are selected from three different fields (Figure 5.1). Reservoir samples are selected from field A and B (Figure 5.1a). Caprock samples are selected from field C (Figure 5.1b).

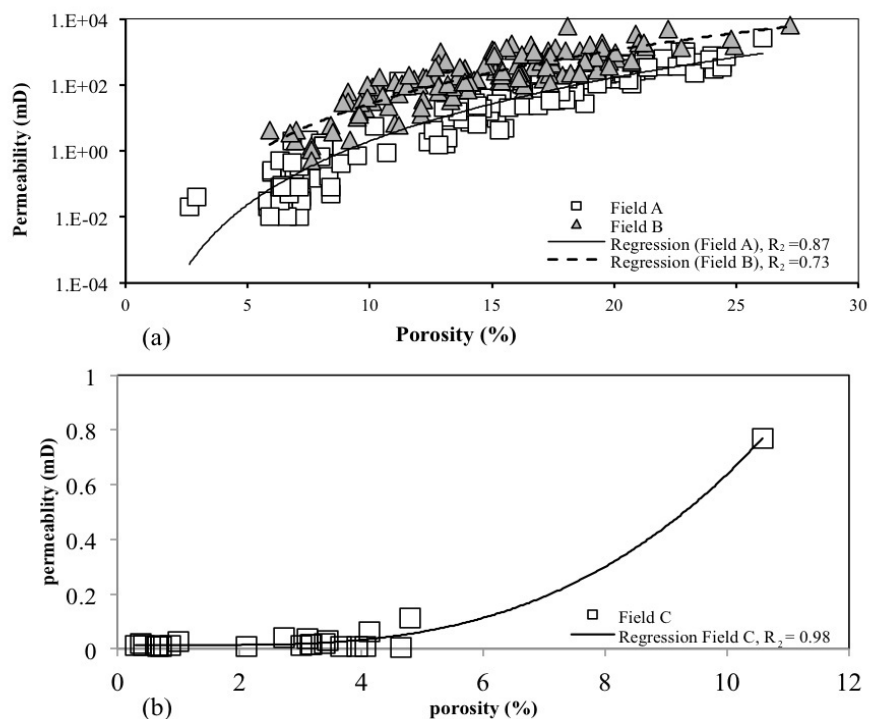


**Figure 5.1** Porosity-permeability relation in three different gas fields. (a) Porosity-permeability relation of the reservoir samples from Field A and Field B. (b) Porosity-permeability relation of the caprock samples from Field C.

Depth, permeability and mineralogy of selected samples are presented in Table 5.1. The permeability measurement and mineralogical analysis techniques are explained in the next section.

**Table 5.1** Initial permeability, depth and mineralogy of the samples. A (reservoir), B (reservoir) and C (caprock) represent the fields from where the samples are selected. Cal= calcite, Dol= Dolomite, Hal= Halite, Qtz= quartz, Kf= K-feldspar, Kao= kaolinite and Alb= Albite. Mineralogy is expressed in wt%.

Sample	Depth (m)	Permeability (mD)	Cal	Dol	Anh	Hal	Qtz	Kf	Kao	Alb
C1	-2905.70	0.059±0.012	0	83.9	15.5	0	0.6	0	0	0
C2	-2895.50	0.007±0.001	0	29.1	70.9	0	0	0	0	0
C3	-2894.50	0.014±0.003	0	1.5	98.5	0	0	0	0	0
C4	-2873.70	0.561±0.084	0	40.4	58.4	0	1.2	0	0	0
C5	-2905.83	0.170±0.025	84.2	8	0.2	3.9	3.7	0	0	0
C6	-2873.55	0.005±0.001	0	44.3	55.7	0	0	0	0	0
B7	-2955.00	460±23	0	3.6	8	0	73.6	13.8	0.5	0.5
A8	-2970.25	0.094±0.019	0	0	3	0.4	85	10	1.6	0
A9	-2983	338±17	0	0	10.7	2.7	83	0	2.9	0.7
B10	-2977.4	218±11	0	1	1	0	95	2	1	0
B11	-2983.1	439±22	0	0	3.8	0	80	7.1	9.1	0
A12	-2909.5	101±5	0	4.8	3.7	6	81	2.5	1.6	0

### 5.2.2 Analytical techniques

Prior to the experiments the mineralogy of the samples was obtained using X-Ray Diffraction (XRD) and Scanning Electron microscopy (SEM) (Table 5.1).

The XRD analysis on the bulk rock samples was performed with Bruker D8 advance (40 Kv, 40 mA). Diffractometers recorded between  $5^{\circ}$  and  $100^{\circ}$  2-Theta with  $\text{Cu}\alpha_1=1.54060 \text{ \AA}$ ,  $\text{Cu}\alpha_2=1.54439 \text{ \AA}$ . The detector step size was set to 0.02 degree with 5 s/step. Use of intact core samples for XRD analysis, rather than in the form of a powder, enabled us to use the same sample for XRD analysis and the experiments, thus linking mineralogy with porosity and permeability. Following the XRD analysis GSAS (General Structure Analysis System) software was used (Larson and Von Dreele, 2004) to quantify different phases in the samples. It should be mentioned that XRD was solely used prior to the experiments for mineralogical analysis.

SEM was performed with a Philips XL-30 environmental SEM (ESEM) with Field Emission Gun (FEG). It is equipped with energy dispersive spectroscopy (EDS). Secondary Electron (SE) and Backscattered Electron (BSE) images were taken on the same location on the core samples before and after the experiments.

Also, before and after the experiments the permeability of the samples was measured with a standard core laboratory permeameter with compressed dry air flowing through the samples at a rate regulated by a calibrated orifice. The measurement error for permeabilities is between 5 and 20% (lower error for higher permeability samples). The details of the permeability measurement method are presented in Bolourinejad and Herber (2014) (Section 2.2.4.1, Figure 2.4).

The porosity of the samples was only measured after the experiments in order to compare the initial porosity-permeability relation with the final one.

Furthermore, before and after the experiments the brine composition was obtained by ICP-OES with a standard deviation of the measured value of less than 3%. Finally the solid residuals precipitated from the brine in the reactor vessels were separated using a centrifuge and subsequently dissolved by hydrofluoric acid and measured by ICP-OES.

### 5.2.3 Experimental setup and procedure

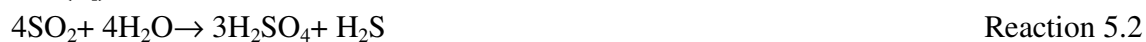
A batch experimental setup with reaction cells has been utilized to create high pressure/high temperature (300 bar and  $100^{\circ} \text{C}$ ) experimental conditions which were equal to those in the subsurface storage sites (Figure 2.3, section 0).

The cylindrical reservoir and caprock core samples with diameter of 25 mm and average thickness of 18 mm were brought in contact with methane (2%) and brine (30 ml), with a composition presented in Table 2.2. The gas mixture ( $\text{CO}_2+100 \text{ ppm H}_2\text{S}+ 100 \text{ ppm SO}_2$ ) was injected to a pressure of 300 bar at a temperature of  $100^{\circ} \text{C}$ . Under these conditions the samples and brine were reacting with the injected gases for a period of 30 days. After completion of the experiment the samples were dried at room temperature.

## 5.3 Results

### 5.3.1 pH and Mineralogy

After injection of CO<sub>2</sub> + 100 ppm H<sub>2</sub>S + 100 ppm SO<sub>2</sub> the pH of the brine was on average reduced from 6.8 to 5.2. This is due to the dissolution of CO<sub>2</sub> and SO<sub>2</sub> in brine and the formation of carbonic and sulphuric acid respectively (Reaction 5.1 and 5.2). Also, dissolution of H<sub>2</sub>S in brine releases H<sup>+</sup> ions which reduce the pH (Reaction 5.3).



It should be mentioned that the pH of the brine after the experiments is a maximum value because of degassing of the gas mixture from brine since the pH was measured under atmospheric conditions.

After injection of the gas mixture typical observations were dissolution of feldspar, carbonate and kaolinite and precipitation of anhydrite. Figure 5.2 represents anhydrite precipitation (Figure 5.2a, b) and dissolution of dolomite (Figure 5.2c, d) and feldspar (Figure 5.2e, f).



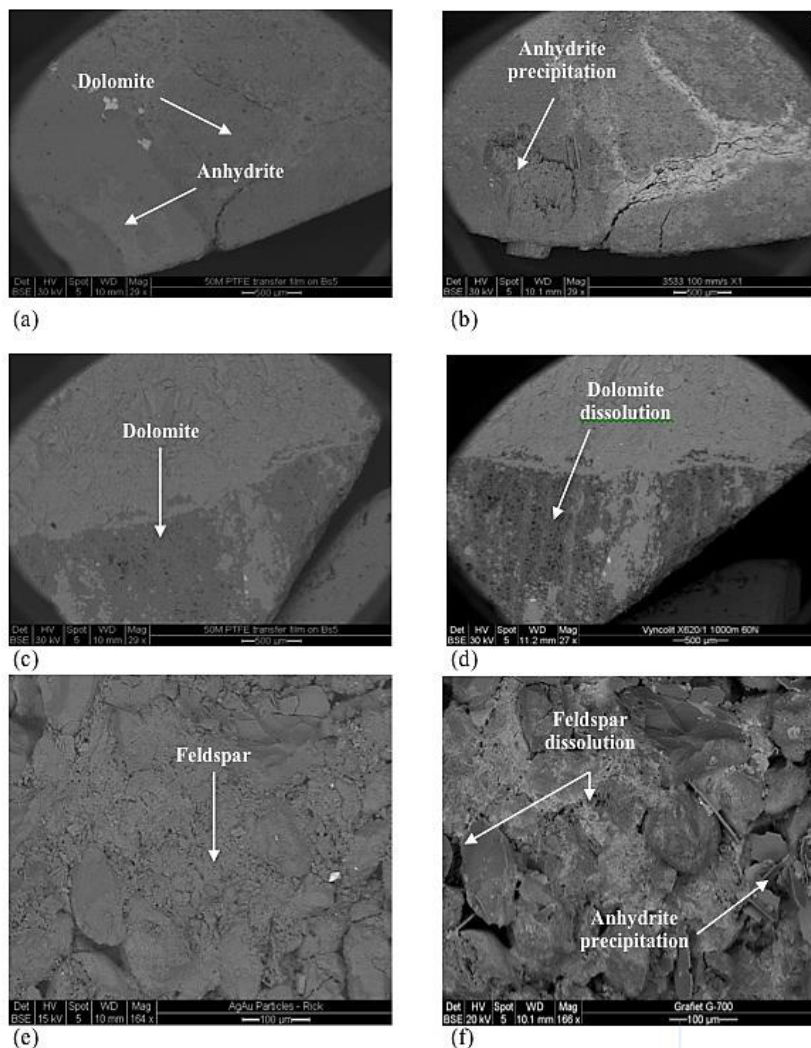


**Figure 5.2** SEM images of Zechstein caprock (a,c) and Rotliegend reservoir samples (e) before the experiment and after (b, d and f)  $\text{CO}_2 + 100 \text{ ppm H}_2\text{S} + 100 \text{ ppm SO}_2$  injection. Before and after images are taken from the same spot on the sample. Anhydrite precipitation (b and f), dolomite dissolution (d) and feldspar dissolution (f) are visible. Please note that images (e) and (f) have a larger magnification.

### 5.3.2 ICP-OES

Upon completion of the experiments the brine samples and solid residuals were analysed with Induced Coupled Plasma- Optical emission Spectroscopy (ICP-OES). The outcome was compared with the ion concentrations in the brine before the experiment (Figure 5.3).

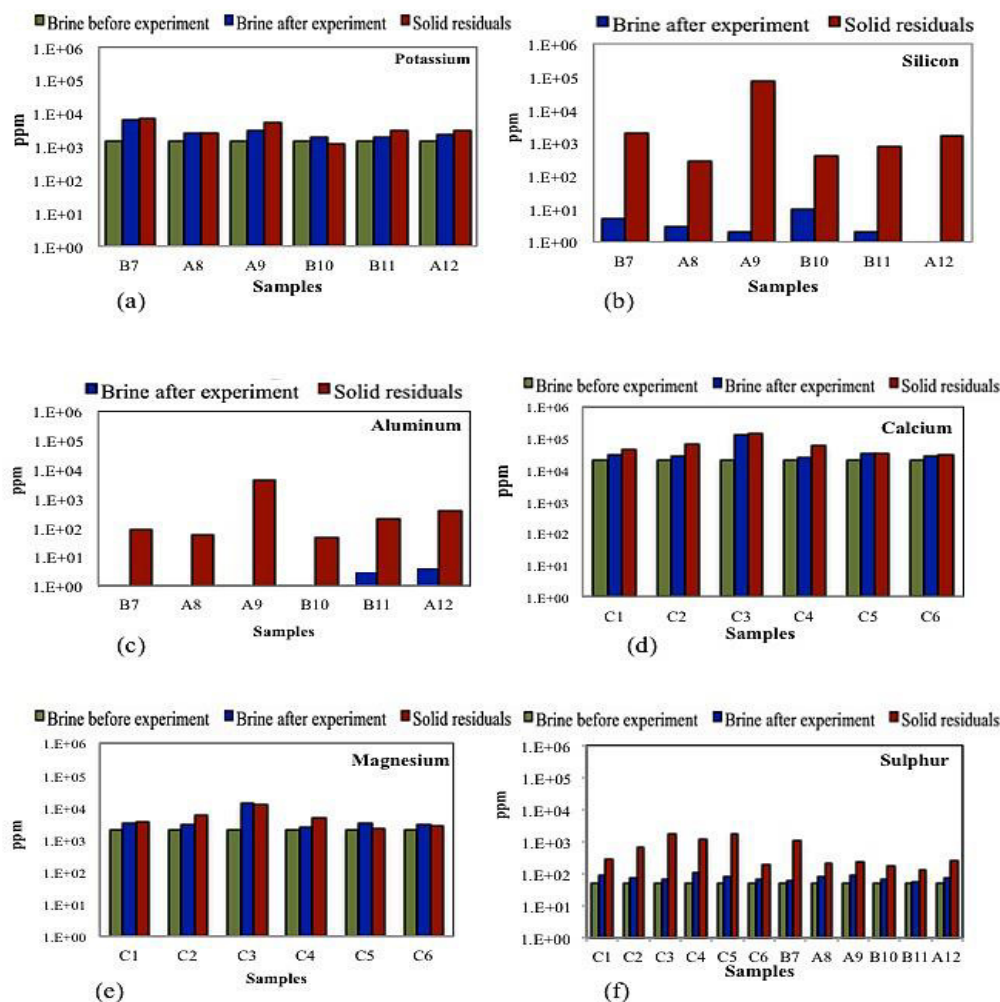


**Figure 5.3.** ICP-OES analysis of the samples. (a) Potassium (b) Silicon (c) Aluminium (d) Calcium (e) Magnesium and (f) Sulphur. In these figures the ion concentration of the samples before the experiment (no initial Si and Al present in the brine) is shown. Also, the brine composition and solid residuals after the experiments is presented. C indicates caprock samples and A, B represent reservoir samples.

In the reservoir samples potassium, silicon and aluminium concentrations are measured. In addition, for caprock samples, the calcium and magnesium concentrations in the brine are compared before and after the experiments. Furthermore, due to the importance of sulphur, this element is measured both in reservoir and caprock samples.

In all cases the concentration of elements in brine and residue increased after the experiment both in reservoir and caprock samples. The increase in Si, K and Al concentrations is caused by the dissolution of silicate minerals like K-feldspar and albite which is confirmed by our SEM analysis. Similarly the rise in Ca and Mg concentration is associated with calcite and dolomite dissolution. The rise in concentration of sulphur in the brine is representative of the dissolution of the sulphur gases ( $H_2S/SO_2$ ). Also, the analysis of solid residues shows presence of sulphur due the precipitation of anhydrite and elemental sulphur.

### 5.3.3 Porosity-permeability

#### 5.3.3.1 Permeability measurements

The permeability of the samples was measured after the experiments in order to assess the effects of mineral dissolution and precipitation on reservoir and caprock properties. In Table 5.2 the permeability of the samples before and after the experiments is compared.

**Table 5.2.** Permeability of the samples before and after the experiments

Sample	Reservoir/caprock	Permeability initial (mD)	Permeability final (mD)	Permeability post/pre
C1	Caprock	0.059±0.012	0.069±0.013	1.2
C2	Caprock	0.007±0.001	0.015±0.003	2.1
C3	Caprock	0.014±0.003	0.033±0.007	2.3
C4	Caprock	0.561±0.084	1.742±0.174	3.1
C5	Caprock	0.170±0.025	3.38±0.338	19.9
C6	Caprock	0.005±0.001	0.015±0.003	3.0
B7	Reservoir	460±23	469±23	1.02
A8	Reservoir	0.094±0.019	0.874±0.131	9.3
A9	Reservoir	338±17	380±19	1.1
B10	Reservoir	218±11	274±14	1.3
B11	Reservoir	439±22	822±41	1.9
A12	Reservoir	101±5	113±6	1.1

In all caprock samples (Field C) the permeability increased by a factor ranging between 1.2 and 3.1 due to the dominance of carbonate mineral dissolution over anhydrite precipitation. The exception is sample C5, which showed an increase in the permeability by a factor of 19.9 due to the presence of micro fractures (Figure 5.2a and Figure 5.2b). These micro fractures contain smaller grain size minerals which dissolve faster. Furthermore, at increasing pressure, fracture propagation may play a role.

In most of the reservoir samples permeability increased by a factor ranging from 1.02 to 1.9. Sample A8 is an anomaly where permeability increased by a factor of 9.3. This sample had the lowest initial permeability and contained more cementing materials such as feldspars. Furthermore, similar to C5, this sample showed a micro fracture.

#### 5.3.3.2 Porosity-permeability relation

The porosity-permeability relation of reservoir and caprock samples was investigated after the experiments since it represents an important input parameter in the simulation studies. Generally, permeabilities in modelling studies are calculated from porosity values (e.g. Bolourinejad et al., 2014; Xu et al., 2007). Hence it is important to assess whether the initial porosity-permeability relationship is still valid after the injection of the gas mixtures. For this purpose the permeability as well as the porosity of the samples was measured after the experiments Figure 5.4.

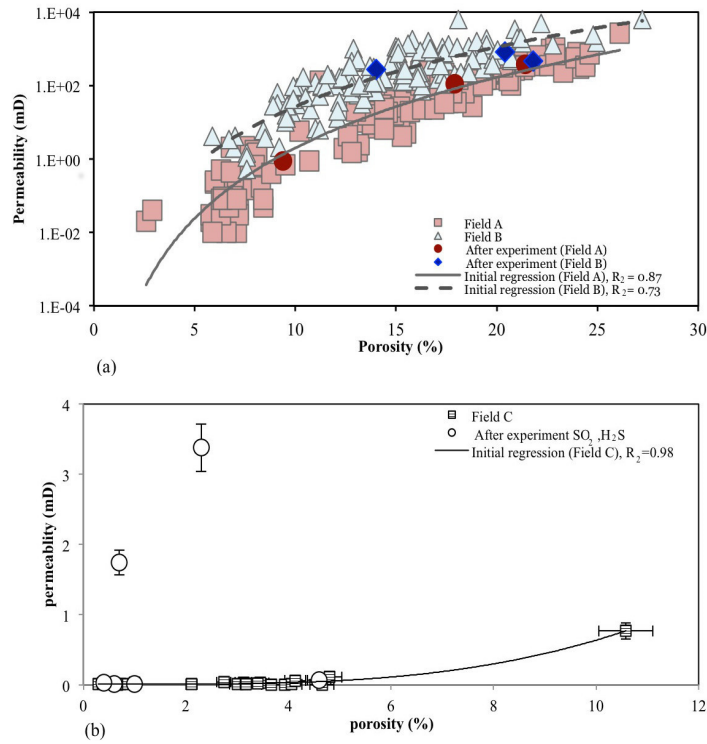


**Figure 5.4** (a) Post experiment porosity-permeability measurements of the reservoir compared to initial porosity permeability relationships for Fields A and B. The measurement error in porosities is 5% and permeabilities between 5% and 20%. (b) Post-experiment porosity-permeability values in comparison with the initial porosity permeability relation of caprock samples.

It is concluded that for the reservoir samples the initial porosity-permeability relation can also be used for post injection scenarios (Figure 5.4a).

For the caprock samples however the results are less conclusive (Figure 5.4b). As discussed earlier, two of the samples contain micro fractures and have therefore anomalously high permeabilities. In the remaining samples the permeabilities are very low, irrespective of porosity which is in the range of 0-5%. It is therefore questionable whether a porosity- permeability trend line is valid for the caprock.

## 5.4 Discussion

The experimental results for injection of a gas mixture (Mixture 1:  $CO_2$ ,  $H_2S$ ,  $SO_2$ ) revealed a variety of mineral reactions. In this section we compare our results with those of an earlier study where similar experiments were performed with a mixture of  $CO_2$  and 100 ppm  $H_2S$  (Mixture 2) only (Bolourinejad and Herber, 2014).

In both cases the acidity of the brine increased dependent on the type of injected components. After injection of mixtures 1 and 2 the initial pH of 6.8 in the brine reduced to 5.2 and 6.1 respectively.  $SO_2$  had the largest impact since its dissolution in brine causes the formation of sulphuric acid which has a larger effect on brine acidity than the

dissolution of  $\text{H}_2\text{S}$ , forming hydrosulphuric acid in brine. The carbonic acid formation by the dissolution of  $\text{CO}_2$  also affects the brine acidity. These effects are illustrated by the acid dissociation constants ( $K_a$ ) for sulphuric, carbonic and hydrosulphuric acids, which are  $1 \times 10^3$ ,  $4.3 \times 10^{-7}$  and  $1 \times 10^{-7}$  respectively.

Another observation is the significant anhydrite precipitation following injection of Mixture 1. Precipitation of this mineral was earlier observed during the experiments with Mixture 2. However, when using Mixture 1 the presence of both sulphur gases provided a larger sulphur source leading to enhanced precipitation of anhydrite (Figure 5.2b).

Of particular interest is the behaviour of kaolinite. In both cases of gas mixture injection dissolution of this mineral was observed to some extent. However, precipitation of kaolinite was only observed after injection of Mixture 2. In the more acidic environment created by presence of both  $\text{H}_2\text{S}$  and  $\text{SO}_2$  (Mixture 1), kaolinite dissolution is dominant over precipitation.

Finally the permeability changes after the injection of these gas mixtures are compared in Figure 5.5.

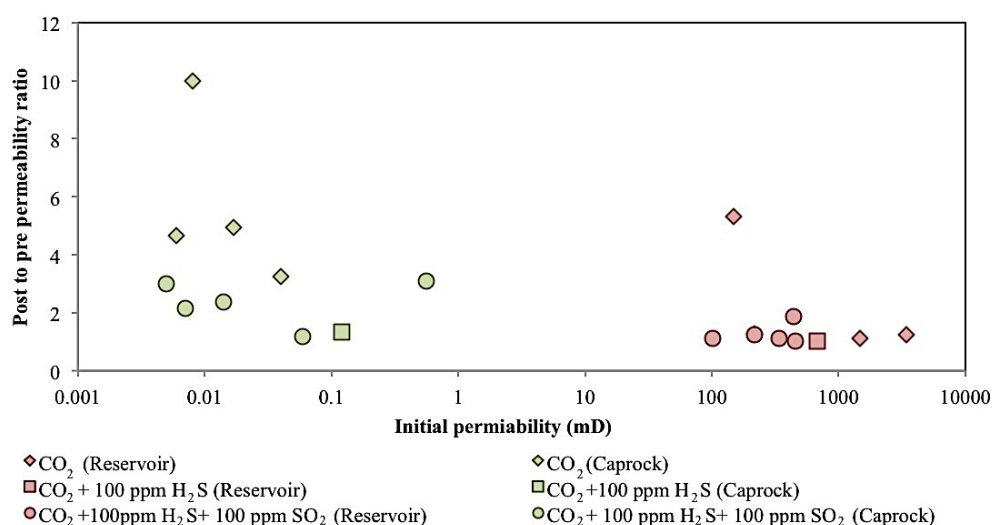


**Figure 5.5** Permeability comparison before and after pure  $\text{CO}_2$ ,  $\text{CO}_2$ + 100 ppm  $\text{H}_2\text{S}$  and  $\text{CO}_2$ + 100 ppm  $\text{H}_2\text{S}$ + 100 ppm  $\text{SO}_2$ . Red and green colours show the reservoir and caprock respectively.

In this figure also the results after injection of pure  $\text{CO}_2$  is incorporated (Bolourinejad and Herber, 2014) as a base case for comparison. Please note that samples C5 and A8 have been omitted from the graph, since they contain micro fractures as discussed above.

Overall, the effect of co-injection of  $\text{H}_2\text{S}$  and  $\text{SO}_2$  with  $\text{CO}_2$  on permeability is within the range of variations caused by injection of  $\text{CO}_2$  with  $\text{H}_2\text{S}$  or pure  $\text{CO}_2$ . In all cases the permeability of the samples has increased.

For the reservoir samples, where initial permeabilities are medium to high, the increase is moderate for all three mixtures and no significant differentiation is observed. In the caprock samples, the much lower initial permeabilities are enhanced by larger factors. From the pattern observed it can be concluded that despite the weaker brine acidity in the

pure CO<sub>2</sub> case, the permeability increase in this set of samples is significantly larger than in those injected with Mixture 1 or 2. In the latter two, the higher acidity led indeed to more mineral dissolution, but this was partly counteracted by enhanced anhydrite precipitation. In the subsurface configuration an increased permeability of cap-rock can lead to increased risk of leakage from underlying reservoirs. However, the resulting increase in the permeability of the caprock is constrained to the bottom of the seal which is in contact with the reservoir. Only when micro-fractures occur in the caprock, the dissolution effect may migrate upward. In tectonic settings where microfractures are observed, the integrity of the caprock seal may be more seriously affected. It should in any case be noted that the initial permeability of the caprock samples in this study is extremely low (less than 0.5 mD) and the post-experiment permeabilities do not exceed 3 mD.

Also, it is worth mentioning that besides the type of impurities in the CO<sub>2</sub> stream also their concentration is an important factor in affecting porosity and permeability of the samples. For example in Bolourinejad and Herber (2014) a comparison has been made between co-injection of 100 ppm and 5000 ppm H<sub>2</sub>S in the CO<sub>2</sub> stream during 30 days experiments. In this article it was stated that “after CO<sub>2</sub>+100 ppm H<sub>2</sub>S injection the permeability remained almost unchanged (slight increase <3%) in the reservoir sample. In the cap-rock samples permeability increased by 30%. However, after CO<sub>2</sub>+ 5000 ppm H<sub>2</sub>S injection, a significant decrease in permeability of both reservoir and caprock samples has been observed”

Although we consider the experimental results as significant, they are constrained by the limitations of some of the measurement techniques.

Firstly, our measurements of sample mineralogy are mainly determined by XRD analysis which is limited to the surface of the rock sample. Possible mineralogical variations within the bulk volume of the sample are therefore not recorded, which might be significant in cases of high heterogeneity in the rock. Although this has been taken into account when macroscopically selecting relatively homogeneous samples, the application of other techniques, such as a combination of SEM and X-ray computed tomography can yield improved determination of the mineralogy.

Secondly, after performing the experiments at reservoir temperature (100°C), the compositional analysis of the brine was performed at room temperature. The cooling of the brine could have led to extra precipitation of some of the dissolved elements, hence affecting their concentration in fluids and solid residuals.

In addition, the experiments were performed in static state in batch reactors. In subsurface reservoirs however the pore-filling fluids and gases are subject to reactive transport conditions due to flow. Further experimentation with flow-through setups is therefore required to corroborate our static results in a dynamic environment.

## 5.5 Conclusion

An experimental study of co-injection of  $\text{CO}_2 + 100 \text{ ppm SO}_2 + 100 \text{ ppm H}_2\text{S}$  in Permian Rotliegend reservoir and Zechstein caprock core samples was performed under subsurface conditions.

Mineral analysis using XRD, SEM and ICP-OES techniques revealed dissolution of carbonate, feldspar and kaolinite minerals after injection of the gas mixture. In addition significant anhydrite and elemental sulphur precipitation occurred due to the presence of sulphur gases.

After the injection of the gas mixture permeability of both reservoir and caprock samples increased in all cases. In the reservoir the effect is moderate with increase factors of 1.02-1.9 and the initial porosity- permeability relationship is preserved after injection. For the caprock the increases are larger, up to a factor of 3.1, but initial permeabilities are low and no meaningful porosity- permeability relationship could be established. In comparison with pure  $\text{CO}_2$  injection the permeability enhancement is less strong due to the precipitation of anhydrites. This may lead to the conclusion that the addition of low quantities (100 ppm) of  $\text{SO}_2$  and  $\text{H}_2\text{S}$  in  $\text{CO}_2$  during subsurface storage does not increase the risk of leakage through the Zechstein caprock more than when using pure  $\text{CO}_2$ . Though these experimental results are encouraging, they need to be complemented with flow-through experiments and reactive transport modelling.